Groot, de J. J. M. C., Veldink, G. A., Vliegenthart, J. F. G., Boldingh, J., Wever, R., & Gelder Van, B. F. (1975) *Biochim. Biophys. Acta 377*, 71–79.
Halliwell, B., & Gutteridge, J. M. C. (1985) in *Free Radicals in Biology and Medicine*, Oxford Science Publications, Oxford, U.K.
Hatzelmann, A., Schatz, M., & Ullrich, V. (1989) *Eur. J. Biochem. 180*, 527–533.
Higgs, G. A., Flower, R. J., & Vane, J. R. (1979) *Biochem. Pharmacol. 28*, 1959–1961.
Kemal, C., Louis-Flamberg, P., Krupinski-Olsen, R., & Shorter, A. L. (1987) *Biochemistry 26*, 7064–7072.
Kühn, H., Holzhütter, H. G., Schewe, T., Hielsch, C., & Rapoport, S. (1984) *Eur. J. Biochem. 139*, 577–583.
Kühn, H., Schewe, T., & Rapoport, S. M. (1986) *Adv. Enzymol. Relat. Areas Mol. Biol. 58*, 273–311.
Kulkarni, A. P., & Cook, D. C. (1988a) *Biochem. Biophys. Res. Commun. 155*, 1075–1081.
Kulkarni, A. P., & Cook, D. C. (1988b) *Res. Commun. Chem. Pathol. Pharmacol. 61*, 305–314.
Lee, W. E., & Miller, D. W. (1966) *Photogr. Sci. Eng. 10*, 192–201.
Lowry, O. H., Roselrough, N. J., Farr., A. L., & Rendell, R. J. (1951) *J. Biol. Chem. 237*, 1375–1376.
Mansuy, D., Cucurou, C., Biatry, B., & Battioni, J. P. (1988) *Biochem. Biophys. Res. Commun. 151*, 339–346.
Mansuy, D., Boucher, J. L., Delaforge, M., & Leclaire, J. (1989) *Biochem. Biophys. Res. Commun. 159*, 1283–1289.
Marnett, L. J., Siedlik, P. H. & Fung, L. W. M. (1982) *J. Biol. Chem. 257*, 6957–6964.
Mulliez, E., Leblanc, J. P., Girerd, J. J., Rigaud, M., & Chottard, J. C. (1987) *Biochim. Biophys. Acta 916*, 13–23.
Nelson, M. J. (1988) *Biochemistry 27*, 4273–4278.
Reynolds, C. H. (1988) *Biochem. Pharmacol. 37*, 4531–4537.
Samuelsson, B., Dahlen, S. E., Lindgren, J. A., Rouzer, C. A., & Serhan, C. N. (1987) *Science 237*, 1171–1176.
Schewe, T., Kühn, H., & Rapoport, S. M. (1986) *Adv. Enzymol. Relat. Areas Mol. Biol. 58*, 192–272.
Slappendel, S., Veldink, G. A., Vliegenthart, J. F. G., Aasa, R., & Malmström, B. G. (1981) *Biochim. Biophys. Acta 667*, 77–86.
Smith, W. L., & Lands, W. E. M. (1972) *J. Biol. Chem. 247*, 1038–1047.
Thang, D. C., Nam, N. H., Chopard, C., Galey, J. B., & Chottard, J. C. (1987) *J. Labelled Compd. Radiopharm. 24*, 297–302.
Van der Zee, J., Eling, T. E., & Mason, R. P. (1989) *Biochemistry 28*, 8363–8367.
Veldink, G. A., Vliegenthart, J. F. G., & Boldingh, J. (1977) *Prog. Chem. Fats Other Lipids 15*, 131–166.
Vliegenthart, J. F. G., & Veldink, G. A. (1982) in *Free Radicals in Biology* (Pryor, W. A., Ed.) Vol. 5, pp 29–64, Academic Press, New York.
Vliegenthart, J. F. G., Veldink, G. A., Verhagen, J., & Slappendel, S. (1983) in *Biological Oxidations* (Sund H., & Ullrich V., Eds.) pp 203–223, Springer-Verlag, Berlin.

Glycolysis and Glucose Uptake in Intact Outer Segments Isolated from Bovine Retinal Rods†

Ricardo Lopez-Escalera,‡ Xue-Bin Li, Robert T. Szerencsei, and Paul P. M. Schnetkamp*
Department of Medical Biochemistry, University of Calgary, Calgary, Alberta T2N 4N1, Canada
Received March 7, 1991; Revised Manuscript Received June 12, 1991

ABSTRACT: Glucose transport across the plasma membrane of isolated bovine rod outer segments (ROS) was measured by uptake of ^{14}C-labeled 3-*O*-methylglucose and 2-deoxyglucose and was inferred from deenergization of ROS with 2-deoxyglucose. Glucose transport was mediated by a facilitated diffusion glucose transporter that equilibrated external and internal free hexose concentrations. Glucose transport in ROS displayed two components as judged from kinetic analysis of hexose equilibration and as judged from inhibition by cytochalasin B and phloretin. Transport under exchange conditions was considerably faster as compared with net hexose uptake, similar to that observed for the erythrocyte glucose transporter. Sensitivity to cytochalasin B and affinity to 3-*O*-methylglucose were similar to those observed for the hepatocyte glucose transporter. The cytochalasin-insensitive component appears unique to ROS and did not reflect leakage transport as judged from a comparison with L-glucose uptake. Glucose transport feeds glycolysis localized to ROS. We suggest that a major role for glycolysis in ROS is phosphorylation of GDP to GTP via pyruvate kinase and PEP, while phosphorylation of ADP to ATP can use the creatine kinase/phosphocreatine pathway as well.

The outer segments of retinal rod cells (ROS) are separated from the rest of the rod photoreceptor cell by a narrow cilium; ROS are the site of visual transduction, both visual excitation and adaptation. The energy demand of ROS arises from the use of GTP by enzymes involved in the metabolism of the excitatory messenger cGMP (i.e., guanylate cyclase and the G-protein transducin) and from the use of ATP for multiple phosphorylation of rhodopsin by rhodopsin kinase and for the reduction of the chromophore retinal to retinol. The metabolic demand in ROS for GTP by enzymes of the cGMP cascade is reflected by the presence in ROS of equimolar concentrations of GTP and ATP (Berger et al., 1980; Biernbaum & Bownds, 1985; Schnetkamp, 1986). It is generally believed that the energy demand of ROS is provided for in its entirety by a dense cluster of mitochondria located in the rod inner

†This research was financially supported by the Canadian Retinitis Pigmentosa Foundation. P.P.M.S. is a scholar of the Alberta Heritage Foundation for Medical Research. R.L.S. was a recipient of a Government of Canada Awards.
*To whom correspondence should be addressed.
‡This paper is dedicated to the memory of Ricardo Lopez-Escalera who sadly passed away on February 21, 1991.

0006-2960/91/0430-8970$02.50/0

segment immediately adjacent to the outer segment. A few earlier studies suggested that ROS have the capability to regenerate ATP via a nonmitochondrial pathway (Schnetkamp, 1981), perhaps involving phosphocreatine and creatine kinase (Dontsov et al., 1978; Schnetkamp & Daemen, 1981). ROS have also been shown to contain phosphotransferases that can shuttle the terminal high-energy phosphate group between adenine and guanine nucleotides (Schnetkamp & Daemen, 1981). Recently, it was reported that glyceraldehyde-3-phosphate dehydrogenase is a major protein associated with the ROS plasma membrane (Hsu & Molday, 1990). Here, we have examined pathways localized to the rod outer segment that are responsible for regeneration of GMP/GDP to GTP and of ADP to ATP; we observed a strong presence of glycolytic enzymes. Consistent with a significant contribution of local glycolysis to ROS energy demands, we observed a facilitated diffusion type glucose transport activity in the ROS plasma membrane.

Materials and Methods

Intact bovine ROS were purified from freshly dissected retinas as described before (Schnetkamp et al., 1979; Schnetkamp, 1986). Bovine eyeballs were purchased from a local abbatoir, and the retinas were dissected as soon as possible. Intact ROS were stored at 4 °C as a concentrated suspension containing 200–300 μM rhodopsin in 600 mM sucrose, 5% (w/v) Ficoll 400, and 20 mM Hepes (the pH of this and all other solutions was adjusted to 7.4 with arginine). For glucose uptake experiments, bovine ROS were diluted with 20 volumes of 200 mM taurine and 20 mM Hepes (pH 7.4) and sedimented at 5000 rpm for 15 min in a Beckman J-20 rotor. The pellet was resuspended in 200 mM taurine and 20 mM Hepes (pH 7.4). Photolysis spectra of intact ROS were recorded as described before (Schnetkamp, 1981).

Enolase, Pyruvate Kinase, and Lactate Dehydrogenase Assays. Lactate dehydrogenase activity was measured by the rate of pyruvate-induced oxidation of NADH monitored at 340 nm. Enolase and pyruvate kinase activity could be measured by coupling to the lactate dehydrogenase assay as well. In order to eliminate possible rate limitation by enzymes placed later in the glycolytic pathway, pyruvate kinase was also assayed in the presence of excess exogenous lactate dehydrogenase, and enolase was also assayed with both exogenous pyruvate kinase and lactate dehydrogenase added in excess. An alternate assay for enolase measured 2-phosphoenolpyruvate (PEP) directly as an increase in light absorption at 240 nm.

Intact ROS were diluted with 100 mM KCl, 5 mM $MgCl_2$, 1 mM dithiothreitol, 70 μM NADH, 20 mM Hepes (pH 7.4), and 0.02% saponin to a final concentration of 1.5–3 μM rhodopsin. Assays were started by addition of the appropriate substrates as described in the text. Recordings were made in an SLM-Aminco DW2C dual-wavelength spectrophotometer in the dual-wavelength mode with the wavelength pair of 340 and 410 nm (NADH oxidation) or 240 and 260 nm (PEP production), respectively, and a slit width of 3 nm. Cuvettes were thermostated via a circulating water bath, and the suspension was mixed with a magnetic spinbar.

Glucose Uptake. Glucose transport activity in the ROS plasma membrane was measured by the uptake of the ^{14}C-labeled 3-*O*-methylglucose or 2-deoxyglucose with a rapid filtration assay over borosilicate glass fiber filters. Intact ROS in the taurine medium (200 mM taurine, 20 mM Hepes, pH 7.4) were incubated at a concentration of 100 μM rhodopsin with ^{14}C-labeled sugars; at the indicated times, aliquots (65 μL) were withdrawn and pipetted into 2.5 mL of ice-cold washing solution (200 mM sucrose, 20 mM Hepes, pH 7.4), and immediately a second portion of 2.5 mL of ice-cold washing medium was added and the filtration started. In earlier experiments, a third portion of 2.5 mL of washing medium was added before the filter ran dry, whereas in later experiments the filter was allowed to run dry before adding the final portion of washing medium. Nonspecific adsorption of the radioisotope was 1.5% in the former procedure and 0.15–0.2% in the latter procedure. Filters were counted in 10 mL of Beckman Ready Protein liquid scintillation cocktail and counted in a Beckman LS 3801 liquid scintillation counter.

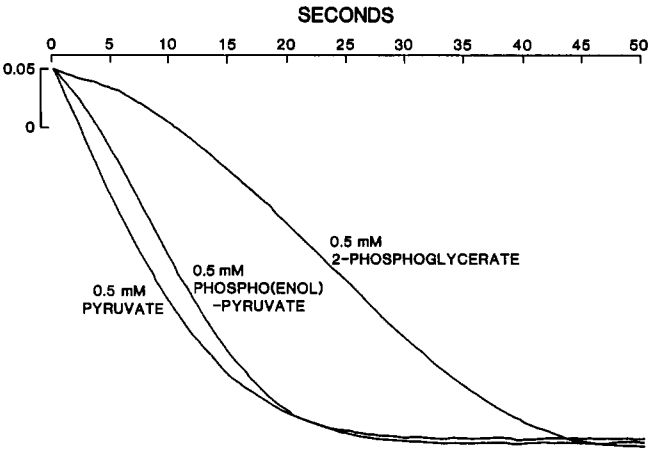

FIGURE 1: NADH oxidation by glycolysis in intact ROS. Intact ROS were incubated in 100 mM KCl, 20 mM Hepes (adjusted to pH 7.4 with arginine), 5 mM $MgCl_2$, 1 mM dithiothreitol, 70 μM NADH, 500 μM ADP, and 0.02% saponin. The final rhodopsin concentration was 1.5 μM. Changes in light absorption were measured in the dual-wavelength mode (340 and 450 nm). Oxidation of NADH was initiated at time zero by addition of 0.5 mM of the indicated glycolytic intermediates. The temperature was 25 °C.

Results

Glycolytic Enzymes in ROS. In earlier studies the presence in ROS of hexokinase (Schnetkamp & Daemen, 1981; Schnetkamp, 1981), lactate dehydrogenase (Futterman et al., 1970), and glyceraldehyde-3-phosphate dehydrogenase (Hsu & Molday, 1990) has been reported. Here, we measured the activity of the three terminal enzymes of anaerobic glycolysis in intact bovine ROS. In order to permeabilize the plasma membrane to solutes, 0.02% saponin was added (in the absence of saponin, about 90% of the enzyme activity was inaccessible to externally added substrate). Figure 1 illustrates the oxidation of NADH by ROS enzymes upon addition of different substrates; NADH oxidation was monitored by a decrease in light absorption at 340 nm. Addition of 0.5 mM pyruvate caused a rapid and complete oxidation of the NADH (70 μM) present to indicate lactate dehydrogenase activity. Addition of 0.5 mM 2-phosphoenolpyruvate (PEP) also caused a rapid oxidation of NADH after a short initial lag phase, but only when ADP or GDP was present; the lag phase indicated the time required to produce pyruvate via the action of pyruvate kinase and could be eliminated by addition of excess exogenous pyruvate kinase. Finally, addition of 0.5 mM 2-phosphoglycerate resulted in the oxidation of NADH (ADP or GDP required), but after a significant lag phase indicating the preceding activity of enolase and pyruvate kinase to produce PEP and pyruvate, respectively. Again, the lag phase observed in the enolase assay employing NADH oxidation could be removed by addition of excess lactate dehydrogenase and pyruvate kinase, whereas no lag phase was observed when the formation of PEP was measured directly at 240 nm. We determined the kinetic properties (V_m and K_m) of all three

enzymes from Lineweaver–Burke plots, which in all cases were linear, indicating single-site saturation kinetics (all values are average ± standard deviation with the number of observations in parentheses). V_m is expressed as a change in overall cytoplasmic concentration per second; the overall rhodopsin concentration in ROS was assumed to be 3 mM. Lactate dehydrogenase had a V_m of 12.6 ± 4.2 mM/s (9) and a K_m for pyruvate of 103 ± 6 μM (4). Pyruvate kinase had a V_m of 15.0 ± 4.6 mM/s (9) and K_m's of 44 ± 17 μM (3) for PEP, 291 ± 72 μM for ADP (9), and 469 ± 129 μM for GDP (8). Enolase had a V_m of 6.6 ± 1.7 mM/s (10) and a K_m for 2-phosphoglycerate of 55 ± 7 μM (5).

Different isoforms of pyruvate kinase have been described (Ibsen, 1977; Hall & Cottam, 1978). The L- and R-type show a sigmoidal dependence on the PEP concentration unlike the Michaelis–Menten kinetics observed in ROS. The M1 and M2 types can be distinguished by the effect of fructose 1,6-diphosphate on the K_m for PEP. No effect of fructose 1,6-diphosphate was observed in ROS (not illustrated) suggesting that bovine ROS contain pyruvate kinase M1 type common in heart, brain, and muscle tissue. Like pyruvate kinase in other tissues, the enzyme in ROS displayed an absolute dependence on K^+ ions (K_m = 80 mM). The V_m of pyruvate kinase from ROS in the presence of K^+ was more than 50-fold larger when compared with its V_m in the presence of either Na^+ or Li^+ (data not illustrated).

PEP and Phosphocreatine as Phosphate Donors for GDP and ADP, Respectively. Considering the unusual circumstance in ROS that concentrations of guanine and adenine nucleotides are of comparable magnitude and considering the unusually high demand for guanine nucleotides by the cGMP cascade, it is noteworthy that pyruvate kinase can phosphorylate both ADP and GDP with comparable efficiency (see above). Intact bovine ROS have been shown to contain both creatine kinase activity (Dontsov et al., 1978; Schnetkamp & Daemen, 1981) and phosphocreatine (Schnetkamp, 1986). We examined the relative ability of PEP and phosphocreatine to phosphorylate ADP and GDP, respectively, in the presence of ROS enzymes. Addition of 1 mM phosphocreatine dramatically decreased both the rate and amount of PEP-induced oxidation of NADH when ADP was the substrate for pyruvate kinase but had no effect when GDP was the substrate. Less oxidation of NADH via glycolysis (pyruvate kinase and lactate dehydrogenase) indicates that ADP (but not GDP) was rapidly phosphorylated to yield ATP via an alternate route (i.e., creatine kinase).

Deenergization of ROS by External 2-Deoxyglucose. In previous paragraphs we described our finding that bovine ROS contain glycolytic enzymes as well as creatine kinase. The presence of these enzymes could explain the observed maintenance of ATP and GTP levels in bovine ROS (Schnetkamp, 1981, 1986). The presence of glycolytic enzymes in ROS suggests that the ROS plasma membrane contains a glucose transporter for import of glucose.

First, we examined the effect of external 2-deoxyglucose on the ability of ROS to utilize endogenous ATP. Endogenous ATP fuels the pentose phosphate pathway that generates the NADPH required for the reduction of *all-trans*-retinal to retinol (Futterman et al., 1970; Schnetkamp, 1981). Photolysis spectra of intact ROS treated with glucose or 2-deoxyglucose are illustrated in Figure 2. In the glucose-treated control, the characteristic 330-nm absorption peak of retinol was observed 25 min after a full bleach, whereas in the presence of 2-deoxyglucose no retinol was observed and the photolysis spectrum was very similar to that observed in lysed ROS membranes. This result suggests that 2-deoxyglucose caused

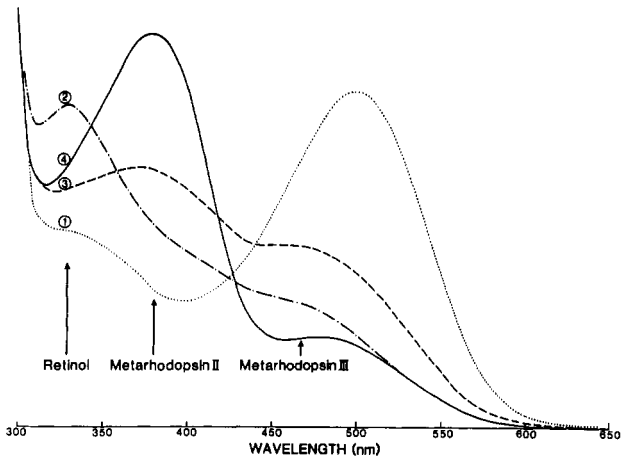

FIGURE 2: Effect of deoxyglucose on retinol formation in intact ROS. Intact ROS were incubated for 5 min prior to illumination in 600 mM sucrose, 20 mM Hepes (adjusted to pH 7.4 with arginine), and 20 mM glucose (spectrum 2) or 20 mM 2-deoxyglucose (spectrum 3). Spectrum 1 represents the unbleached ROS; spectrum 4 was recorded 10 s after bleaching 80% of the rhodopsin present; spectrum 3 was recorded 30 min after a 80% bleach with deoxyglucose present; spectrum 2 was recorded 30 min after a 80% bleach with glucose present. The arrows indicate the photoproducts retinol, metarhodopsin II, and metarhodopsin III, respectively. The temperature was 25 °C.

the complete depletion of endogenous ATP, most likely because 2-deoxyglucose entered the ROS cytoplasm via a hexose carrier and was subsequently phosphorylated by hexokinase, yielding 2-deoxyglucose-6-phosphate, a metabolic dead end.

The absolute K^+ requirement of pyruvate kinase enabled us to test the route via which ATP is regenerated in intact ROS as judged by the rate and amount of reduction of retinal to retinol. In the presence of the channel ionophore gramicidin, we can replace internal K^+ by other alkali cations, such as Li^+, which cannot activate pyruvate kinase. We compared the effect of gramicidin and Li^+ (to inhibit pyruvate kinase) on the rate of retinol formation with that observed with gramicidin and K^+ (to stimulate pyruvate kinase) and observed little difference in the initial rate of retinol formation and at most a 20% drop in the amount of retinol formed in 1 h (not illustrated). We interpret this finding to indicate that ATP regeneration in intact ROS is not necessarily mediated via the K^+-dependent pyruvate kinase but can occur via a K^+-independent process, most likely via creatine phosphate/creatine kinase (see above).

Glucose Uptake by Purified Bovine ROS. Deenergization of isolated ROS by external 2-deoxyglucose (Figure 2) strongly suggests the presence of a glucose transporter in the ROS plasma membrane. Direct evidence for glucose uptake was obtained by measuring the uptake of ^{14}C-labeled 3-*O*-methylglucose and 2-deoxyglucose into ROS with a rapid filtration technique. A rapid uptake of 3-*O*-methylglucose with a half-time of about 15 s was observed at 25 °C, but not at 0 °C (Figure 3; the ordinate intercept of 1.5% represented nonspecific absorption to the filters). A second slow phase of 3-*O*-methylglucose uptake was observed at both 0 and 25 °C. Uptake of 2-deoxyglucose proceeded to significantly higher levels than that observed for 3-*O*-methylglucose (Figure 3, compare inverted triangles with triangles), most likely caused by phosphorylation of internalized 2-deoxyglucose in the ROS cytoplasm.

Glucose transporters in other cell types mediate either facilitated diffusion transport that equilibrates hexose concentrations or Na^+-dependent uphill transport. Glucose transport in ROS was not dependent on external Na^+. Equilibrium uptake of ^{14}C-labeled 3-*O*-methylglucose in the experiment

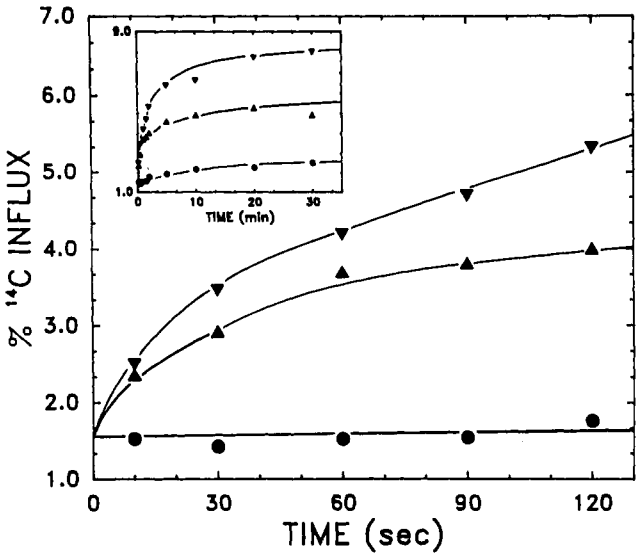

FIGURE 3: Hexose uptake by intact ROS. Intacted ROS were incubated in 200 mM taurine and 20 mM Hepes (adjusted to pH 7.4 with arginine) to a final rhodopsin concentration of 138 μM. Uptake of ^{14}C-labeled 3-*O*-methylglucose (triangles and circles) and 2-deoxyglucose (inverted triangles), respectively, was initiated at time zero by addition of radioisotope and 0.25 mM of the "cold" sugar. The temperature was 25 °C (triangles and inverted triangles) or 0 °C (circles). The insert shows hexose uptake on a time scale of 30 min. Sugar uptake is expressed as the percentage of the total amount of ^{14}C-labeled sugar added.

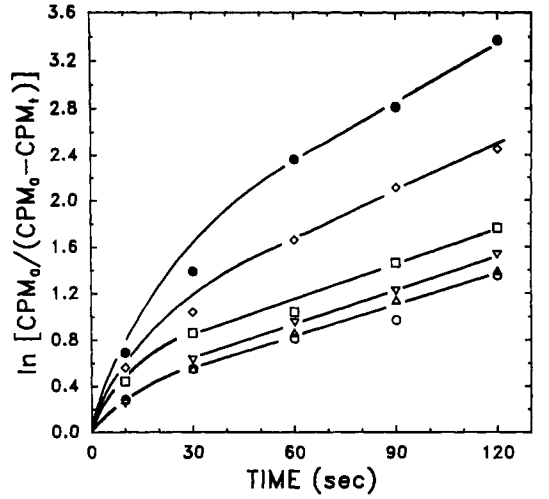

FIGURE 4: Kinetic analysis of hexose efflux and exchange in intact ROS. Intact ROS were equilibrated with 1 mM 3-*O*-methylglucose and ^{14}C-labeled 3-*O*-methylglucose for 30 min at a rhodopsin concentration of 416 μM. Efflux was initiated at time zero by 40-fold dilution in 200 mM taurine, 20 mM Hepes (adjusted to pH 7.4 with arginine), and 3-*O*-methylglucose (3-*O*-methylglucose replaced an equimolar amount of taurine from the medium): 0 mM (open circles), 1 mM (triangles), 10 mM (inverted triangles), 25 mM (squares), 50 mM (diamonds), and 100 mM (filled circles). The initial uptake level was 13% of the total amount of radioactivity added. CPM_0 represents initial uptake level, whereas CPM_t represents counts that remain incorporated after t seconds of efflux. A monoexponential efflux curve should fit the equation: $CPM_t = CPM_0e^{-kt}$, where k is the rate constant. The temperature was 25 °C.

illustrated in Figure 3 amounted to 3.4% of the total amount present. On the assumption that the overall rhodopsin concentration in ROS is 2 mM in our hypotonic medium, the volume of ROS in this experiment amounted to 6.9% of the total suspension volume, suggesting that 3-*O*-methylglucose had access to 51% of the total ROS volume, a reasonable value for the contribution of ROS cytosol to total ROS volume. In nine different ROS preparations the equilibrium uptake of ^{14}C-labeled 3-*O*-methylglucose indicated that the sugar had access to 62% (SD = 7) of the total internal volume of ROS. Consistent with a facilitated diffusion type glucose transporter, we observed that the equilibrium uptake of ^{14}C-labeled 3-*O*-methylglucose was independent of the concentration of cold 3-*O*-methylglucose present in the range of 1–100 mM (not illustrated).

Glucose Uptake in ROS Displays Two Kinetic Components. Uptake of ^{14}C-labeled 3-*O*-methylglucose by facilitated diffusion into a single compartment should display a monoexponential uptake curve (Gliemann, 1989). However, we never observed a monoexponential curve for the equilibration of 3-*O*-methylglucose in ROS, indicating that uptake displayed at least two kinetic components (not illustrated). Two kinetic components were also suggested by analysis of ^{14}C-labeled 3-*O*-methylglucose efflux. Equilibrium uptake of ^{14}C-labeled 3-*O*-methylglucose in a concentrated ROS suspension was followed by dilution with sugar-free medium or with media containing increasing concentrations of cold 3-*O*-methylglucose (Figure 4). Efflux with a single rate constant is expected to yield a straight line when the logarithm of the fraction of radiolabeled hexose remaining is plotted against time (Gliemann, 1989). In ROS, efflux patterns displayed a distinct biphasic pattern suggesting at least two kinetic components. Increasing the concentration of 3-*O*-methylglucose in the efflux medium increased the amount of ^{14}C-labeled 3-*O*-methylglucose that was released with rapid kinetics from 26% with no sugar added to 73% with 100 mM 3-*O*-methylglucose present in the efflux medium. The rapid component of net entry (e.g., Figure 3) was compared with the rapid component of net exit, both at a concentration of 1 mM 3-*O*-methylglucose. In nine preparations net influx in 10 s amounted to 27% (SD = 7) of the equilibrium uptake, whereas in seven preparations net efflux amounted to 26% (SD = 6) of total internal sugar.

Net Entry versus Exchange Transport. The efflux experiment illustrated in Figure 4 suggests that exchange transport is considerably faster than net transport and has a K_m for 3-*O*-methylglucose in the tens of millimolar. We examined uptake of ^{14}C-labeled 3-*O*-methylglucose as a function of the external "cold" 3-*O*-methylglucose concentration under conditions that (1) net entry was measured (Figure 5, filled symbols) or that (2) exchange transport was measured after previous equilibration with cold sugar (Figure 5, open symbols). At a concentration of 1 mM "cold" 3-*O*-methylglucose, net entry and exchange uptake of ^{14}C-labeled 3-*O*-methylglucose were quite similar. "Cold" 3-*O*-methylglucose was much more effective in reducing the rate of net ^{14}C-labeled 3-*O*-methylglucose uptake when compared with exchange ^{14}C-labeled 3-*O*-methylglucose uptake. This indicates that (1) the K_m for net uptake is considerable lower than that for exchange uptake and that (2) the V_m for exchange uptake is considerably greater than that for net uptake. The kinetic parameters (K_m and V_m) of the initial rate of both exchange and net uptake were obtained from Eadie–Hofstee plots. To obtain an approximation of the initial rate of hexose transport, the first two time points were averaged, and the results were expressed in uptake of sugar molecules/(ROS·s). Consistent with the observations illustrated in Figure 4, both the K_m and the V_m for exchange uptake were found to be greater than those of net uptake: the average V_m and K_m for exchange uptake amounted to 3.4×10^6 hexose molecules/(ROS·s) (SD = 1.5×10^6) and 38 mM (SD = 15), respectively (five preparations), whereas the average V_m and K_m for net uptake amounted to 1.0×10^6 hexose molecules/(ROS·s) (SD = 0.7

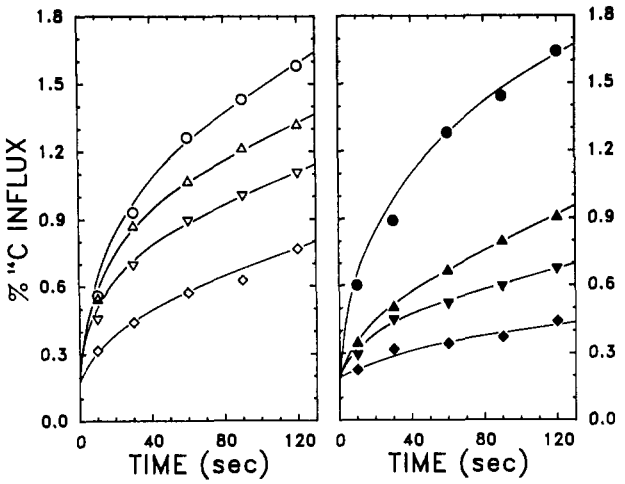

FIGURE 5: Net uptake and exchange uptake via the hexose carrier in ROS. Uptake of ^{14}C-labeled 3-*O*-methylglucose as a function of "cold" 3-*O*-methylglucose concentration was measured as described in the legend of Figure 3 (3-*O*-methylglucose replaced an equimolar amount of taurine from the medium). Exchange uptake (left panel, open symbols) was measured by equilibration of ROS with "cold" 3-*O*-methylglucose for 30 min prior to addition of ^{14}C-labeled 3-*O*-methylglucose; net uptake (right panel, filled symbols) was measured by simultaneous addition of "cold" 3-*O*-methylglucose and ^{14}C-labeled 3-*O*-methylglucose. 3-*O*-Methylglucose concentrations were 1 mM (circles), 10 mM (triangles), 25 mM (inverted triangles), and 100 mM (diamonds). The temperature was 25 °C.

$\times 10^6$) and 10 mM (SD = 7), respectively (six preparations). A rate of 3.4×10^6 molecules/(ROS·s) equates to a rate of 0.13 mol of hexose per mol of rhodopsin per second or a change in overall concentration of 0.38 mM s^{-1}. On the assumption that the cytoplasm comprises about 50% of the total ROS volume, the hexose carrier can change cytoplasmic hexose concentrations by about 0.76 mM s^{-1}.

Inhibition of Glucose Transport in Bovine ROS. Facilitated diffusion type glucose transporters in other cell types are selectively inhibited by phloretin and cytochalasin B. In the experiments illustrated in Figure 6, we examined the effect of both drugs on efflux of ^{14}C-labeled 3-*O*-methylglucose efflux when ROS preloaded with the labeled sugar were diluted 45-fold with sugar-free medium. Reducing the temperature to 0 °C was the most effective inhibitor of ^{14}C-labeled 3-*O*-methylglucose efflux. Phloretin caused inhibition of most of the efflux, but a small efflux component persisted even at very high phloretin concentrations (Figure 6A). Application of cytochalasin B revealed a similar picture of two efflux components, one very sensitive to cytochalasin B and fully inhibited at a few micromolar concentration of the drug, whereas a second component was not inhibited, even at very high drug concentrations (Figure 6B). To ensure that the cytochalasin-insensitive component did not reflect passive leakage, we measured uptake of 3-*O*-methylglucose in the presence of cytochalasin B and compared it with L-glucose uptake (Figure 7). The cytochalasin-insensitive component of uptake was considerably greater when compared with L-glucose uptake or 3-*O*-methylglucose uptake at 0 °C and on a longer time scale appeared to approach the same level as observed in the absence of cytochalasin B.

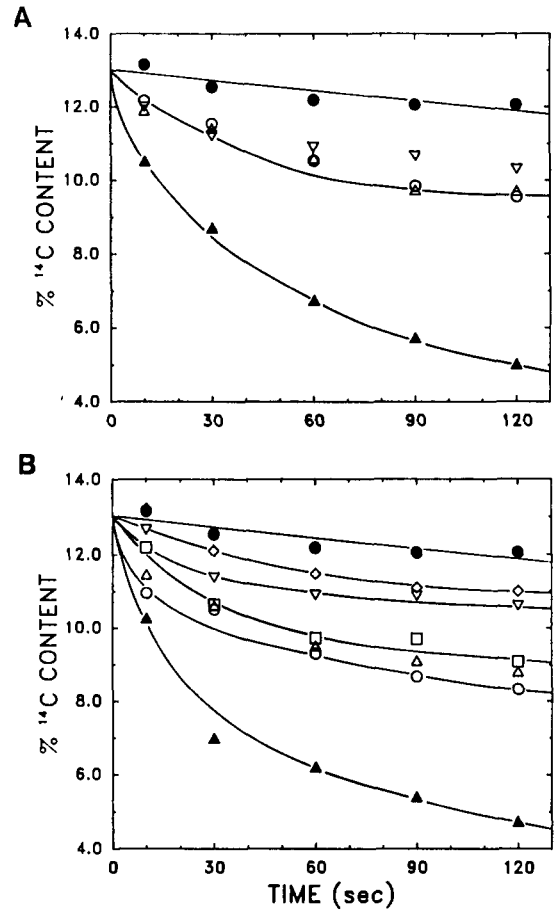

FIGURE 6: Inhibition of hexose transport in ROS by cytochalasin B and phloretin. The efflux of preequilibrated ^{14}C-labeled 3-*O*-methylglucose was measured at 25 °C (except for filled circles) as described in the legend of Figure 4. The efflux conditions were (A) no additions and 0 °C (filled circles); no additions (filled triangles); 50 μM phloretin (open circles); 100 μM phloretin (open triangles); 500 μM (inverted triangles); and (B) 0 °C and no additions (filled circles); no additions (filled triangles); cytochalasin B (open symbols), 0.5 μM (circles), 1 μM (triangles), 5 μM (squares), 20 μM (inverted triangles), 100 μM (diamonds).

Discussion

A Glucose Transporter in the ROS Plasma Membrane. Our results demonstrate that the plasma membrane of isolated intact bovine ROS contains a glucose transporter of the facilitated diffusion type, capable of maximal transport of 3.4×10^6 hexose molecules/(ROS·s). Equilibrium uptake levels of ^{14}C-labeled 3-*O*-methylglucose suggested that the glucose transporter equilibrated hexose concentrations across the ROS plasma membrane in the entire population of ROS (Figure 3 and its discussion). Both cytochalasin-sensitive and cytochalasin-insensitive hexose uptake appeared to have access to the entire population of ROS (Figure 7). This provides a strong argument against the possibility that either form of hexose uptake occurs in only a minor fraction of particles in the suspension (e.g., ROS with the inner segment still attached and the glucose transporter located in the inner segment plasma membrane). In a similar vein, addition of 2-deoxyglucose abolished reduction of retinal to retinol in the entire population of ROS (Figure 2). Finally, addition of mitochodrial uncouplers such as FCCP has no effect on ATP levels in isolated ROS, suggesting that the ROS ATP pool is not in contact with mitochondria (Schnetkamp, 1981, 1986). The above three lines of evidence strongly suggest that glucose uptake is a property of the ROS plasma membrane and cannot be accounted for by inner segment contamination.

The maximal rate of change in cytoplasmic hexose concentration at 25 °C under exchange conditions was a cytoplasmic change of hexose concentration by 0.76 mM s^{-1}. This value is lower than that observed for erythrocytes (6 mM s^{-1}), higher than that observed for adipocytes in the absence of insulin (0.1 mM s^{-1}), and comparable to that observed for

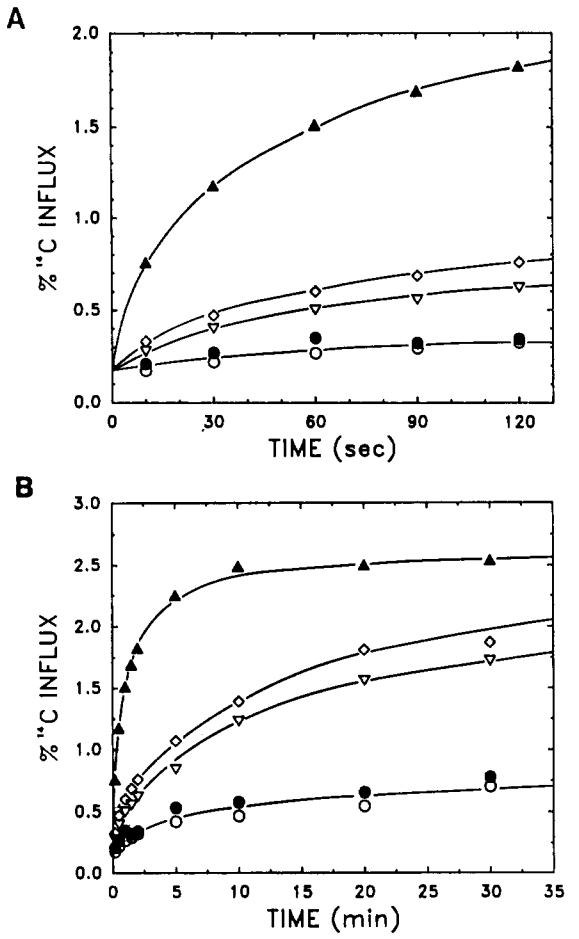

FIGURE 7: Effect of cytochalasin B on hexose influx. The influx of ^{14}C-labeled 3-*O*-methylglucose and ^{14}C-labeled L-glucose was measured at 25 °C as described in the legend of Figure 3. Shown are 1 mM 3-*O*-methylglucose with no additions (filled triangles); 10 μM cytochalasin B (open diamonds); 100 μM cytochalasin B (open inverted triangles); L-glucose replaces 3-*O*-methylglucose (open circles); 0 °C (filled circles).

adipocytes in the presence of insulin (1 mM s^{-1}) (Gliemann & Rees, 1983).

Utilization of Glucose for Regeneration of ATP and GTP in ROS. The presence of a glucose transporter in the ROS plasma membrane suggests the presence of glycoloysis localized to ROS. Regeneration of high-energy phosphates in ROS appeared to occur via two pathways, glycolysis (pyruvate kinase, both ADP and GDP) and phosphocreatine/creatine kinase (ADP only). A significant portion of ADP regeneration in ROS could take place via the latter pathway. Phosphocreatine probably functions as a the main high-energy shuttle between inner and outer segment. We suggest that an important function of glycolysis in ROS lies in the rapid phosphorylation of GDP to GTP, necessitated by the high concentration of guanine nucleotides in ROS and to support the GTPase activity of transducin and the guanylate cyclase.

Kinetics of Hexose Transport in ROS. It might be anticipated that ROS express the Glut1 brain/erythrocyte glucose transporter. However, the kinetic properties of the ROS hexose transporter observed in this study appear different from those found for the erythrocyte glucose transporter but instead appear a curious mixture of properties of different glucose transporters in different tissues. The greater rate of exchange transport as compared with net uptake is reminiscent of the erythrocyte glucose transporter and unlike the insulin-sensitive adipocyte transporter [reviewed by Gliemann and Rees (1983)]. The high K_m value for 3-*O*-methylglucose and the relative insensitivity to cytochalasin B (inhibition in the low micromolar range as opposed to the submicromolar range) are reminiscent of the transporter found in hepatocytes (Axelrod & Pilch, 1983) and in the islets of Langerhans (Johnson et al., 1990). In addition, the ROS hexose transporter displayed some perhaps unique features, most noticeably the presence of a cytochalasin-insensitive component of 3-*O*-methylglucose uptake and the extremely low activity at 0 °C. A considerable uptake of D-glucose insensitive to cytochalasin B was also observed in liver plasma membrane vesicles, but this uptake appeared to reflect nonspecific leakage since uptake of L-glucose was equally large under these conditions (Axelrod & Pilch, 1983). In contrast, cytochalasin-insensitive glucose uptake in ROS greatly exceeded uptake of L-glucose or uptake of 3-*O*-methylglucose at 0 °C (Figure 7). With respect to cation transport, the ROS plasma membrane has been demonstrated to be extremely well-sealed, and cation fluxes are carried exclusively by the Na–Ca–K exchanger (Schnetkamp, 1989; Schnetkamp et al., 1991).

The coexistence of functionally distinct glucose transporters has recently been demonstrated in rat kidney on the basis of immunofluorescence (Thorens et al., 1990) as well as in adipocytes on the basis of kinetic analysis (Whitesell et al., 1989). In both cases one glucose transporter displayed a high affinity (1 mM) and the other a low affinity (>50 mM) for glucose, both inhibitable by cytochalasin B. In the case of ROS, non-monoexponential kinetics could suggest uptake into two different compartments, or it could suggest that the kinetic parameters of hexose transport change during the time-course of uptake or efflux. The latter possibility is more consistent with our observation that the amount of internal hexose accessible to the rapid efflux component was not constant but varied with the external hexose concentration (Figure 4). During the time course of ^{14}C-labeled 3-*O*-methylglucose uptake, the ratio of net uptake/exchange uptake continuously changed and, since both uptake modes displayed different kinetic parameters, monoexponential kinetics are not expected. Equilibration of ^{45}Ca and ^{86}Rb via the self-exchange mode of the ROS Na–Ca–K exchanger displayed monoexponential kinetics suggesting that bovine ROS represent a homogeneous preparation with respect to this protein (Schnetkamp, 1980, 1989; Schnetkamp et al., 1991). Cytochalasin-insensitive and cytochalasin-sensitive hexose transport both appeared to equilibrate hexose concentrations into the same compartment since hexose transport in the presence of 10 or 100 μM cytochalasin B proceeded at about the same rate and appeared to equilibrate at the same level observed in the absence of cytochalasin B (Figure 7). It is therefore possible that two functionally different glucose transporters are present in the ROS plasma membrane. Alternatively, a cytochalasin-resistant conformation of the ROS hexose transporter may exist. More detailed experiments on the kinetic properties of glucose transport in ROS, on binding of cytochalasin B to ROS, and on the type of glucose transporter(s) that are expressed in the retina are under way in our laboratory to establish the place of the ROS glucose transporter among those found in other tissues.

Registry No. 5′-ATP, 56-65-5; 5′-GTP, 86-01-1; 5′-ADP, 58-64-0; 5′-GDP, 146-91-8; glucose, 50-99-7; pyruvate kinase, 9001-59-6; enolase, 9014-08-8; lactate dehydrogenase, 9001-60-9; pyruvic acid, 127-17-3; phosphoenolpyruvate, 138-08-9; 2-phosphoglyceric acid, 2553-59-5; phosphocreatine, 67-07-2.

REFERENCES

Axelrod, J. D., & Pilch, P. F. (1983) *Biochemistry 22*, 2222–2227.

Berger, S. J., DeVries, G. W., Carter, J. G., Schulz, D. W., Passonneau, P. N., Lowry, O. H., & Ferendelli, J. A. (1980) *J. Biol. Chem. 255*, 3128-3133.
Biernbaum, M. S., & Bownds, M. D. (1985) *J. Gen. Physiol. 85*, 83-105.
Dontsov, E. A., Zak, P. P., & Ostrovskii, M. A. (1978) *Biochemistry (Moscow) 43*, 471-474.
Futterman, S., Hendrickson, A., Bishop, P. E., Rollins, M. H., & Vacano, E. (1970) *J. Neurochem. 17*, 149-156.
Gliemann, J. (1989) *Methods Enzymol. 173*, 616-634.
Gliemann, J., & Rees, W. D. (1983) *Curr. Top. Membr. Transp. 18*, 339-379.
Hall, E. R., & Cottam, G. R. (1978) *Int. J. Biochem. 9*, 785-793.
Hsu, S.-C., & Molday, R. S. (1990) *J. Biol. Chem. 265*, 13308-13313.
Ibsen, K. H. (1977) *Cancer Res. 37*, 341-353.
Johnson, J. H., Newgard, C. B., Milburn, J. L., Lodish, H. F., & Thorens, B. (1990) *J. Biol. Chem. 265*, 6548-6551.
Schnetkamp, P. P. M. (1980) *Biochim. Biophys. Acta 598*, 66-90.
Schnetkamp, P. P. M. (1981) *Biochemistry 20*, 2449-2456.
Schnetkamp, P. P. M. (1986) *J. Physiol. 373*, 25-45.
Schnetkamp, P. P. M. (1989) *Prog. Biophys. Mol. Biol. 54*, 1-29.
Schnetkamp, P. P. M., & Daemen, F. J. M. (1981) *Biochim. Biophys. Acta 672*, 307-312.
Schnetkamp, P. P. M., Klompmakers, A. A., & Daemen, F. J. M. (1979) *Biochim. Biophys. Acta 552*, 379-389.
Schnetkamp, P. P. M., Szerencsei, R. T., & Basu, D. K. (1991) *J. Biol. Chem. 266*, 198-206.
Thorens, B., Lodish, H. F., & Brown, D. (1990) *Am. J. Physiol. 259*, C286-C294.
Whitesell, R. R., Regen, D. M., & Abumrad, N. A. (1989) *Biochemistry 28*, 6937-6943.

Preparation and Characterization of Spin-Labeled Derivatives of Epidermal Growth Factor (EGF) for Investigations of the Interactions of EGF with Its Receptor by Electron Paramagnetic Resonance Spectroscopy†

Lee Anne Faulkner-O'Brien,‡ Albert H. Beth,§ Ioannis A. Papayannopoulos,‖ P. S. R. Anjaneyulu,‡,⊥ and James V. Staros*,‡

Department of Biochemistry and Department of Molecular Physiology and Biophysics, Vanderbilt University, School of Medicine, Nashville, Tennessee 37232, and Department of Chemistry, Massachusetts Institute of Technology, Cambridge, Massachusetts 02139

Received January 9, 1991; Revised Manuscript Received May 22, 1991

ABSTRACT: We prepared, purified, and characterized derivatives of epidermal growth factor (EGF) having a nitroxide spin-label attached covalently at the amino terminus. Characterization of these derivatives with regard to the positions of attachment of the spin-label was accomplished by a combination of peptide mapping, protein sequencing, and fast atom bombardment–mass spectrometry. One derivative was chosen for use in initial investigations by electron paramagnetic resonance (EPR) spectroscopy of receptor-bound EGF and its dissociation kinetics. This derivative was found to be equipotent with the native hormone in competitive binding assays, in activating the EGF receptor kinase, and in stimulating the formation of EGF receptor dimers in solubilized cell extracts. Upon binding to solubilized EGF receptor, the spin-labeled EGF derivative became immobilized, giving rise to a visually distinct slow-motion EPR spectrum. The resulting spectrum showed no detectable dipolar interaction between nitroxides, indicating that the nitroxide moieties of spin-labels reacted at the amino termini of receptor-bound spin-labeled EGF molecules are separated by a distance of at least 16 Å. An EPR study of the kinetics of dissociation of spin-labeled EGF in the presence of excess unlabeled EGF revealed a rapid component with a $k_{off} \approx 2 \times 10^{-2}$ s^{-1} and a less well resolved slow component.

EGF[1] was initially purified from murine submandibular glands on the basis of its property of promoting early eyelid opening in newborn mice (Cohen, 1962). It has since been shown to modulate cell growth and differentiation in a variety of target tissues (Carpenter & Cohen, 1979; Carpenter 1981). The receptor for EGF [for reviews, see Carpenter (1987),

† This work was supported by Grants PO1 CA43720, S10 RR04075, and T32 GM07347 from the National Institutes of Health. The mass spectrometry was carried out at the MIT Mass Spectrometry Facility, funded by a grant from the National Institutes of Health (RR00317 to Prof. K. Biemann). A preliminary account of some of this work was presented at the 1989 Annual Meeting of the Biophysical Society (Faulkner et al., 1989).

* Address correspondence to this author at his present address: Department of Molecular Biology, Vanderbilt University, Box 1820, Station B, Nashville, TN 37235.
‡ Department of Biochemistry, Vanderbilt University.
§ Department of Molecular Physiology and Biophysics, Vanderbilt University.
‖ Department of Chemistry, Massachusetts Institute of Technology.
⊥ Present address: Department of Cellular, Molecular and Structural Biology, Morton Building no. 4-672, Northwestern University Medical School, 320 East Superior St., Chicago, IL 60611.

[1] Abbreviations: Asp-N, endoproteinase Asp-N; BSA, bovine serum albumin; BS^3, bis(sulfo-*N*-succinimidyl)suberate; BSSDP, bis(sulfo-*N*-succinimidyl)doxyl-2-spiro-4′-pimelate; EGF, epidermal growth factor; mEGF, murine EGF as purified by the method of Savage and Cohen (1972); EGFα, the 53-residue intact form purified from mEGF; EGTA, ethylene glycol bis(β-aminoethyl ether)-*N*,*N*,*N*′,*N*′-tetraacetic acid; EPR, electron paramagnetic resonance; FAB, fast atom bombardment; HEPES, *N*-(2-hydroxyethyl)piperazine-*N*′-2-ethanesulfonic acid; HPLC, high-performance liquid chromatography; k_{off}, kinetic dissociation constant; $NaDodSO_4$, sodium dodecyl sulfate; PMSF, phenylmethanesulfonyl fluoride; PTH, phenylthiohydantoin; SSTPOC, sulfo-*N*-succinimidyl-2,2,5,5-tetramethyl-3-pyrolin-1-yloxy-3-carboxylate; TEA, triethylamine; TFA, trifluoroacetic acid; V_1, first-harmonic, in-phase, absorption EPR signal.

0006-2960/91/0430-8976$02.50/0